

# Robust Deep Learning for Eye Fundus Images: Bridging Real and Synthetic Data for Enhancing Generalization

Guilherme C. Oliveira<sup>a,b</sup>, Gustavo H. Rosa<sup>a</sup>, Daniel C. G. Pedronette<sup>a</sup>, João P. Papa<sup>a</sup>, Himeesh Kumar<sup>c</sup>,  
Leandro A. Passos<sup>a</sup>, Dinesh Kumar<sup>b</sup>

<sup>a</sup>*School of Sciences, São Paulo State University, São Paulo, Brazil*

<sup>b</sup>*School of Engineering, Royal Melbourne Institute of Technology, Victoria, Australia*

<sup>c</sup>*Centre of Eye Research, University of Melbourne, Victoria, Australia*

---

## Abstract

Deep learning applications for assessing medical images are limited because the datasets are often small and imbalanced. The use of synthetic data has been proposed in the literature, but neither a robust comparison of the different methods nor generalisability has been reported. Our approach integrates a retinal image quality assessment model and StyleGAN2 architecture to enhance Age-related Macular Degeneration (AMD) detection capabilities and improve generalizability. This work compares ten different Generative Adversarial Network (GAN) architectures to generate synthetic eye-fundus images with and without AMD. We combined subsets of three public databases (iChallenge-AMD, ODIR-2019, and RIADD) to form a single training and test set. We employed the STARE dataset for external validation, ensuring a comprehensive assessment of the proposed approach. The results show that StyleGAN2 reached the lowest Fréchet Inception Distance (166.17), and clinicians could not accurately differentiate between real and synthetic images. ResNet-18 architecture obtained the best performance with 85% accuracy and outperformed the two human experts (80% and 75%) in detecting AMD fundus images. The accuracy rates were 82.8% for the test set and 81.3% for the STARE dataset, demonstrating the model's generalizability. The proposed methodology for synthetic medical image generation has been validated for robustness and accuracy, with free access to its code for further research and development in this field.

**Keywords:** Medical images, Age-Related Macular Degeneration, Data Augmentation, Deep Learning, Generative Adversarial Networks, StyleGAN2.

---

## 1. Introduction

Deep learning (DL) techniques are suitable for automated analysis of medical images and have been shown to outperform experts in several fields. Examples of applications of such approaches are to perform discriminative retinal image analysis, such as automated classification of fundus images for detection of referable diabetic retinopathy [1, 2, 3, 4, 5], retinopathy of prematurity [6], exudates on the retina [7], and age-related macular degeneration (AMD) [8, 9, 10], and also for granular AMD severity classification [11, 12]. However the potential of this approach for medical images is limited because they require a large

---

*Email addresses:* gc.oliveira@unesp.br (Guilherme C. Oliveira), gustavo.rosa@unesp.br (Gustavo H. Rosa), daniel.pedronette@unesp.br (Daniel C. G. Pedronette), joao.papa@unesp.br (João P. Papa), himeesh@gmail.com (Himeesh Kumar), leandro.passos@unesp.br (Leandro A. Passos), dinesh@rmit.edu.au (Dinesh Kumar)

number of annotated images that are not currently available. It is also essential that the datasets should be balanced to avoid biased training. Usually, annotated medical image data sets are not sufficiently large nor balanced, and this is often due to issues of privacy of medical data [13].

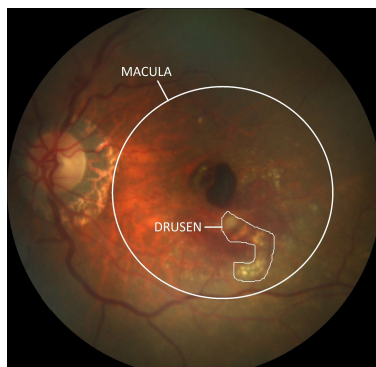


Figure 1: Retina fundus image positive to age-related macular degeneration identified by the presence of drusen. The image was extracted from the iChallenge-AMD dataset [14].

Different approaches have been used to address this shortcoming such as transfer learning using previously trained models, and data augmentation [15, 16]. Brigato et al. [17] highlight the value of standard data augmentation techniques, such as cropping, rotation, and color jittering, as well as using low-complexity convolutional neural networks for small datasets. However, they suggest the development of more complex data generation and augmentation pipelines. Spatial transformations, while adding images, do not guarantee data variability [18], and pre-trained networks often face limitations due to being trained in different learning domains.

A promising solution to generate synthetic images lies in the Generative Adversarial Networks (GANs) [19]. Such an approach performs data augmentation by competitively creating new samples, i.e., a generator attempts to create synthetic images to fool the discriminator, which then tries to identify whether they are fake or real. GANs have also provided exceptional results over a wide variety of medical applications, such as liver lesion classification [20], Barrett’s esophagus identification [21, 22], and chest pathology recognition [23]. However, these did not address problems with generalization, where there is a variable quality and other differences in images of the dataset.

In the field of Optical Coherence Tomography (OCT) imaging, super-resolution GANs (like ESR-GAN [24]) have demonstrated their value as a tool to enhance the quality of the image and improve AMD detection [25]. Das et al. [26] proposed a quick and reliable super-resolution approach concerning OCT imagery using GANs, achieving a classification accuracy of 96.54%.

In retinal imaging, GANs have been used to create synthetic data. Li et al. [27] highlighted the importance of enhancing the quality of synthetic retinal images in their review, emphasizing that using synthetic images in training can improve performance and help mitigate overfitting. Bellemo et al. [28] described the possible advantages and limitations towards synthetic retina image generation using GANs. The authors highlighted the potential clinical applications of GANs concerning early- and late-stage AMD classification. Burlina et al. [8] trained a Progressive GAN [29] on 133,821 color fundus images from 4,613 age-related eye disease individuals to learn how to generate synthetic fundus images with and without AMD. Two retina specialists were asked to distinguish between images with and without AMD for original and synthetic images. Recognition rates varied from around 84% for the first specialist to about 89% for the second. The accuracy differences between synthetic and real images did vary slightly for both specialists.

While the outcomes show great potential, the authors did not verify the utilization of data augmentation during the training process with their approach. Furthermore, Burlina et al. [8] conducted their research using the Age-Related Eye Disease Study (AREDS) dataset. This dataset mainly includes participants from the United States, making it reflective of a North American demographic.

Anh et al [30] tested the FundusGAN to generate eye-fundus images for two eye disease: Age-related macular degeneration and Diabetic retinopathy and demonstrated its ability for the synthetic images to be generalisable for the two disease. However, Anh et al. [30] work was confined to a single dataset in which most participants were from India and lacked diversity. Thus, they could not evaluate their technique across different ethnicities, demographics, and equipment variations, and therefore, their study could not be tested for generalisability.

StyleGAN2 has been utilized to generate detailed images of the eye fundus. Mayya et al. [31] performed data augmentation with StyleGAN2. They developed a method to diagnose a range of conditions such as myopia, diabetic retinopathy, age-related macular degeneration, glaucoma, and cataract. Meanwhile, Wang et al. [32] employed a distinct approach using StyleGAN2 and augmentation, categorizing conditions into four classes: no AMD, early AMD, intermediate AMD, and advanced AMD. However, Mayya et al. [31] and Wang et al. [32] didn't specify a method for removing images with significant quality issues, such as those that are blurry, have low contrast, or are inadequately illuminated. Veturi et al. [33] conducted a diagnostic study focusing on gene-labeled fundus autofluorescence (FAF) images for inherited retinal diseases (IRDs). However, They found that synthetic data augmentation failed to enhance disease classification when applied to IRD datasets.

Age-related macular degeneration (AMD) is a major cause of vision impairment and has affected approximately 200 million people worldwide in 2020 [34]. With an aging population, such numbers are expected to rise to 288 million by 2040 [35]. AMD is a progressive disorder of the macular region that causes central vision loss and is one of the most common causes of irreversible vision impairment in people over 50 years-old [36]. Figure 1 depicts an example of a retina fundus affected by AMD.

This work has introduced an alternative approach for generating synthetic images for training deep networks and tested it for AMD identification, which consists in using a retinal image quality assessment model [37] and the StyleGAN2-ADA [38]. Retina images, positive and negative to AMD, from multiple databases having a range of image qualities and lesions were used. Ten different GAN architectures were compared to generate synthetic eye-fundus images and the quality was assessed using the Fréchet Inception Distance (FID), two independent clinical experts who were label blinded and deep-learning classification. Different percentages of synthetic data were employed in the augmentation.

The primary contributions of this work are fourfold:

- To introduce StyleGAN2-ADA [38] for eye fundus image generation;
- Test generalization across different datasets;
- Free access to software for generating the synthetic images;
- Accessible web-based tool for diagnosing AMD that combines computer vision and deep learning techniques.

The remainder of this paper is organized as follows. Section 2 presents methodology. Section 3 describes the experimental results and Section 5 states conclusions and future works.

## 2. Methodology

This section describes the datasets that were used in the study, the techniques employed to generate the synthetic images, and the methodology to evaluate the different neural architectures considered in the experimental section.

### 2.1. Dataset

This study used eye-fundus images from four public datasets from four countries which have been reported in the literature. These capture the typical differences due to equipment and demographics, which is necessary for verifying the generalisability of the data. Below, we summarized the datasets' preliminary information:

- **iChallenge-AMD:** Comprises of 1,200 retinal fundus images that have been annotated for drusen and hemorrhage. The training set was made of 400 images (89 images of eyes with AMD and 311 from eyes without AMD), while the test sets contained the remaining images [14].
- **ODIR-2019:** Contains colored fundus images from both left and right eyes of 5,000 patients obtained from multiple hospitals/medical centers in China, with varying image resolutions and observations from several specialists. The dataset has been designed to address normal and six diseases: diabetes, glaucoma, cataract, AMD, hypertension, myopia, and other diseases/abnormalities<sup>1</sup>. The training set is made up of a structured dataset with 7,000 images, of which 280 images are labelled as having AMD. The testing set consists of 500 colored fundus images, eliminating age and gender.
- **RIADD:** contains 3,200 fundus images recorded using 3 different cameras and multiple conditions. The images have been annotated through the consensus of two retina experts. The dataset has been sub-divided based on six diseases/abnormalities; diabetic retinopathy, AMD, media haze, drusen, myopia, and branch retinal vein occlusion [39]. The dataset was subdivided into three subsets: 60% for training (1,920 images), 20% for validation (640 images), and the remaining 20% for testing purposes (640 images).
- **STARE:** STructured Analysis of the REtina (STARE), contains 400 high-quality fundus images with different diseases.<sup>2</sup> We randomly sampled 40 AMD and 40 normal images from STARE for testing our model. This database was not part of the mix that was used to train the model and hence testing the model from images from this database was a test for its generalisability. All the ground truths are annotated by the expert.

We have used publicly available and online datasets, each of which have described their patient recruitment, clinical outcomes and human experiments ethics approval in their associated publications. Registration was necessary for access to the data from the three sources.

i-Challenge dataset authors confirm in their publications they received ethics approval guidelines from Sun-Yat Sen University, China and Sixth People's Hospital Affiliated to Shanghai Jiao Tong University, Shanghai, China. Details on <https://amd.grand-challenge.org/Home/>

ODIR dataset confirm that all data is from routine clinical examinations, have been de-identified and published after receiving clearance from Peiking University board. Details on <https://odir2019.grand-challenge.org/dataset/>

---

<sup>1</sup><https://odir2019.grand-challenge.org/dataset/>

<sup>2</sup><https://cecas.clemson.edu/~ahoover/stare/>

RIADD dataset confirms that data collection was conducted after ethics approval from Review Board of Shri Guru Gobind Singhji Institute of Engineering and Technology, Nanded, India. Details on <https://riadd.grand-challenge.org/>

The datasets mentioned above were designed to address a challenge and hence the labels of the test subset were not available. Therefore, we used only the training subset.

These datasets have an imbalanced class distribution, which is an inherent problem for most medical image datasets and using such a set generally leads to a bias towards the predominant class. Different research groups have developed these datasets with differences in the quality of the images and the demographics. Thus, these datasets offered both, data imbalance and wide range of image quality.

The ODIR-2019 and RIADD datasets were organized into two subsets, AMD and non-AMD images. Preprocessing methodology and quality classification was same as proposed by Fu et al. [37], which comprises of a step that detects the retinal mask using the Hough Circle Transform and then crops it to remove the impact of the black background. The cropped region was then scaled to a  $224 \times 224$  resolution. The resultant images were submitted to a DenseNet trained by Fu et al. [37] which classified these in 3 classes: “Good”, “Usable” and “Reject”. The rejected images were of poor quality based on significant blurring, low contrast, inadequate illumination, which has been described by Fu et al. [37]. As a result, the number of images positive to AMD decreased from 89 to 74, 280 to 227, and 100 to 79 images in the iChallenge-AMD, ODIR-2019, and RIADD datasets, respectively while the number of non-AMD images decreased from 311 to 290, 6,720 to 4,993, and 1,820 to 1,143 images concerning the iChallenge-AMD, ODIR-2019, and RIADD datasets, respectively. Figure 2 illustrates the steps mentioned above for a sample image from the ODIR-2019 dataset.

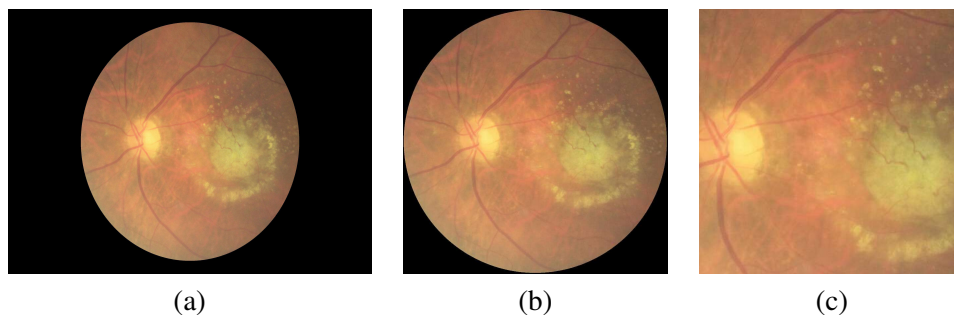


Figure 2: Sample image extracted from ODIR-2019 dataset and its corresponding transformations: (a) original image, (b) background removal using Hough Circle Transform and resizing, and (c) central cropping.

These images were then resampled to  $390 \times 390$  pixels, followed by a cropping procedure keeping the center of the image to  $256 \times 256$  pixels. Such a procedure is required to drive StyleGAN2-ADA generating images focused on the macula area (Figure 2-c). Ultimately, images were resized  $224 \times 224$  pixels and normalized within the range  $[-1, 1]$  to be used as proper inputs to the deeper architectures considered in the manuscript.

After quality assessment and selecting the images for the final dataset using the criterion described earlier, the resulting single dataset comprised total of 7,106 images. In this, 6,896 images were used to train the models (275 with AMD and 6,621 without AMD) and the remaining 210 images (105 with AMD) were used as a holdout test set. Figure 3 displays the number of images used per dataset to compose the final test set.

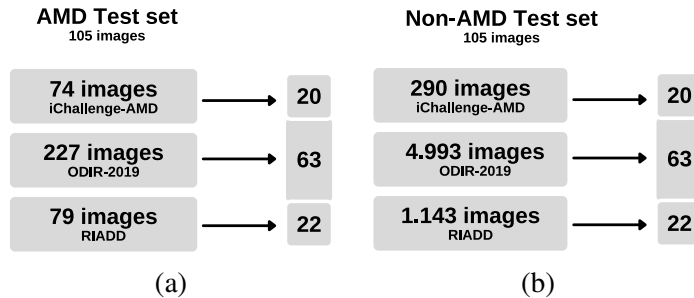


Figure 3: Number of images per dataset to compose the test set: (a) images positive to AMD and (b) non-AMD images.

## 2.2. Evaluation Measures

Evaluating the quality of synthetic images is important for establishing their usability in practical applications, such as training deep learning models. It can significantly influence the training of these models. If the data does not accurately represent reality or lacks diversity, the synthetic data may introduce noise into the training, decreasing the model performance.

We employed three evaluation measures, i.e., the Fréchet Inception Distance (FID), a well-known GAN evaluation score [40], the ability of human experts to identify the synthetic images and the classification accuracy. FID is often used to assess the quality and variety of the generated images and, even though it has been proposed to improve the standard Inception Score, it still uses the Inception architecture to extract features from both, synthetic and real images.

Structural Similarity Index (SSIM), and Peak Signal-to-Noise Ratio (PSNR) focus on pixel-wise comparisons and are limited in their capacity to assess higher-level features and perceptual quality. FID leverages the features extracted from a pre-trained Inception Network to measure the similarity of feature representations between real and generated images.

## 2.3. Experimental Setup

There were four stages of the experiments: (i) comparison of ten different GAN architectures, (ii) evaluation of synthetic images based on human experts’ ability to distinguish between real and synthetic images, (iii) evaluation of data augmentation with synthetic images in three different deep learning networks, and (iv) measuring the accuracy in identifying AMD images between human experts and deep learning networks trained with mixed data, with both real and synthetic images.

The first experiment employed FID to compare StyleGAN2-ADA and nine distinct GAN models. The following models were considered in the experiment: Deep Convolutional GAN (DCGAN) [41], Least Squares Generative Adversarial Networks (LSGAN) [42], Wasserstein GAN (WGAN) [43], Wasserstein GAN with Gradient Penalty (WGAN-GP) [44], Deep Regret Analytic Generative Adversarial Networks (DRAGAN) [45], Energy-based Generative Adversarial Network (EBGAN) [46], Boundary Equilibrium Generative Adversarial Networks (BEGAN) [47], Conditional GAN (CGAN) [48], and Auxiliary Classifier GAN (ACGAN) [49]. All models were trained with 50 epochs, considering samples of size  $100 \times 100$  pixels and a batch size of 32. The training step used the ADAM[50] optimizer with a learning rate of 0.0002 and decay rates of 0.5 and 0.999 regarding the generator and the discriminator, respectively. The experiments were conducted using the training set with an Nvidia RTX 2060 GPU. Therefore, after training each GAN model, new images were generated and FID was computed.

The second experiment determines whether clinical experts, who are very experienced with the analysis of eye fundus images, can distinguish between synthetic and real images. Such a step is essential to evaluate the effectiveness of StyleGAN2-ADA for generating synthetic eye fundus images. The experts were

provided with randomly generated image sets, one for AMD-diagnosed images and the other for non-AMD images, each consisting of ten synthetic images and ten real images. They were asked to identify the synthetic images in the mix.

In the next experiment, we considered three deep architectures pre-trained with ImageNet dataset [51] for performance comparison when the model is augmented with synthetic images, i.e., SqueezeNet [52], AlexNet [53], and ResNet18 [54]. During training, synthetic and real images were mixed within each batch according to a pre-determined hyperparameter  $p \in [0, 1]$ . For each image, a uniform distributed number  $x$  was sampled and compared with  $p$ : if the latter was greater than  $x$ , the image was replaced by a synthetic one. We considered images generated by StyleGAN2-ADA, for it had obtained the best FID values in the first experiment (such outcomes are later described in Section 3). The deep networks were trained using a learning rate of 0.0001, a decay rate of 0.9, batch size of 32, number of epochs equal to 5, and samples of size  $224 \times 224$  pixels.

To address the issue of unbalanced dataset, Weighted Random Sampler [55] was used. This approach can be implemented in PyTorch [56]. It assigns weights to each data point in the dataset. These weights are inversely proportional to the class frequency to which they belong. When batches of data are drawn for training the model during the training process, this sampler uses these weights to influence the selection process, making it more likely for points from minority classes to be included in each batch. Further augmentation was performed using classical image transformations, such as resizing and color jittering, which changes the brightness, contrast, saturation, and horizontal flipping. The test set was kept intact.

The final round was aimed at comparing the best deep model obtained in the previous phase, ResNet-18, against human experts concerning the task of AMD identification. In this step, twenty real images (ten AMD images and ten non-AMD images) were randomly selected from the test set and provided to human experts for classification purposes. Following that, the same images were submitted to a ResNet-18 for comparison purposes. To allow a fair comparison between humans and deep models, we considered the following measures: standard accuracy (ACC), sensitivity, and specificity.

In this work, we used the StyleGAN2-ADA official source code, and the hyperparameters suggested by Karras et al. [38]. Concerning StyleGAN2-ADA hyperparameters, we used a batch size of 12, ADA target equal to 0.8 (i.e., the probability of using ADA mechanism), the Adam algorithm with a learning rate of 0.0025, decay values of 0 and 0.99, and a convergence error of  $1e^{-8}$  for the generator and discriminator. StyleGAN2-ADA framework enables different augmentations (rotation, geometric transformations, and color transformations) and class-conditional training. The output image resolution was set to  $256 \times 256$  pixels.

### 3. Results

The experimental results are presented in four sub-sections: (i) FID for synthetic image assessment, (ii) human experts detecting synthetic images, (iii) data augmentation assessment, (iv) comparison between human experts and deep models for detecting AMD images, and (v) web-based tool to access and validate the deep learning method model.

#### 3.1. Synthetic Image Assessment

Table 1 presents the FID values for each GAN-based architecture. StyleGAN2-ADA achieved the lowest FID value of 166, while EBGAN was placed in last and its FID value of 380 was the highest. The smaller the FID value, the better is the quality of the generated image. Therefore, all further experiments only considered the StyleGAN2-ADA architecture for synthetic image generation.

Table 1: Mean FID values for image quality assessment (the best result is highlighted in bold).

Type	Architecture	FID
Unconditional	EBGAN	380.18
	DCGAN	326.85
	DRAGAN	317.82
	WGAN	307.00
	LSGAN	305.59
	WGAN-GP	295.23
	BEGAN	225.89
Conditional	CGAN	342.59
	ACGAN	315.36
	<b>StyleGAN2-ADA</b>	<b>166.17</b>

Figure 4 shows a comparison between (a) real images from the training dataset and (b) synthetic images produced by StyleGAN2-ADA. The trained model yields realistic-looking images for both, with and without AMD, conditioned by sampling from latent representations. Visual inspection shows that the generated images are similar to the real images. In the AMD images, macula degeneration is evident.

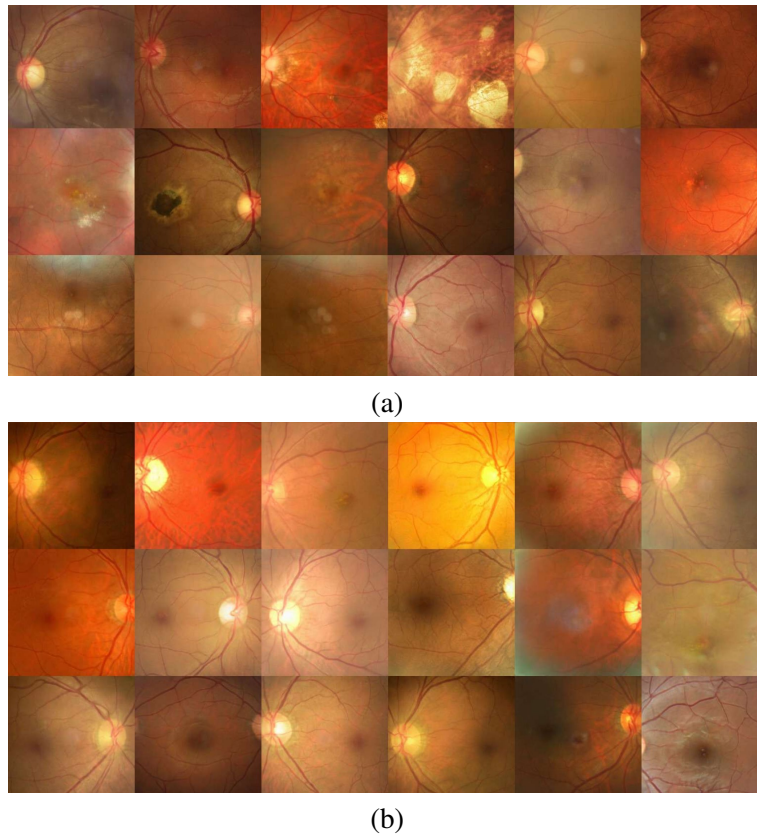


Figure 4: Examples of (a) real retina images extracted from the training dataset, and (b) synthetic images generated by StyleGAN2-ADA.

Figure 5 provides examples of real and synthetic images that are from eyes, positive and negative to



AMD. One can observe the high-quality images that were generated for both, AMD and non-AMD images.

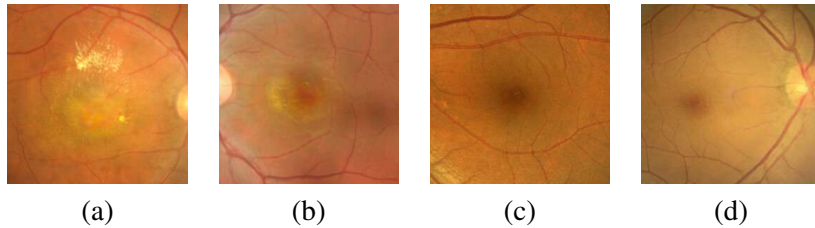


Figure 5: Examples of synthetic and real images for AMD and Non-AMD. (a) real, positive AMD, (b) synthetic, positive AMD, (c) real, Non-AMD and (d) synthetic, non-AMD.

### 3.2. Distinguishing between Synthetic and Real Images

Table 2 presents the outcomes of each clinical expert. For AMD images, the accuracy was 50% (standard deviation of 21.91%) for clinician #1 and 55% (standard deviation of 21.80%) for clinician #2. For Non-AMD images, clinician #1 achieved an accuracy of 60% (standard deviation of 21.47%), and clinician #2 obtained an accuracy of 50% (standard deviation of 21.47%). These results highlight that both clinicians could not differentiate between real and synthetic images.

Table 2: Synthetic versus real images by humans experts.

		ACC	Sensitivity	Specificity
AMD	<b>Clinician #1</b>	0.50	0.50	0.50
	<b>Clinician #2</b>	0.55	0.40	0.70
Non-AMD	<b>Clinician #1</b>	0.60	0.60	0.60
	<b>Clinician #2</b>	0.50	0.40	0.60

### 3.3. Data Augmentation Assessment

In this study we performed on-the-fly data augmentation during training. Figure 6 shows the accuracy over the test set concerning different percentages ( $p$  value) of real images that were replaced by synthetic images. Overall, the accuracy improved when combining synthetic and real images. While the accuracy lies between 50% and 55% when using only synthetic images, and between 78% and 81% when using only real images for training, the combination of both types of images gave the best results. However, this was network dependent: while SqueezeNet accuracy peaked at 81% when using 70% of synthetic images, AlexNet obtained its highest accuracy (82%) when using only 20% of synthetic images. ResNet18 achieved its best of 83% with 60% of synthetic images. In general, the networks performed poorly when the percentage of synthetic images exceeded 70%.

Figure 6(b) shows the accuracy over the test set using only real ( $p = 0$ ) and also mixed data concerning ResNet18, AlexNet, and SqueezeNet architectures. The most significant improvement was by AlexNet, its accuracy increased by approximately 8%, while ResNet18 had highest accuracy (about 83%) using a mix of synthetic and real images.

### 3.4. Comparison between Human Experts and Deep Models

Table 3 presents the comparison of AMD detection by human experts, SqueezeNet, AlexNet and Resnet-18. Overall, the results of both clinicians and deep-learning were similar, with the best performance by deep-learning while the lowest specificity was by clinician #2. This shows that deep models are at least as good, and may outperform clinicians for diagnosing AMD in eye fundus images.

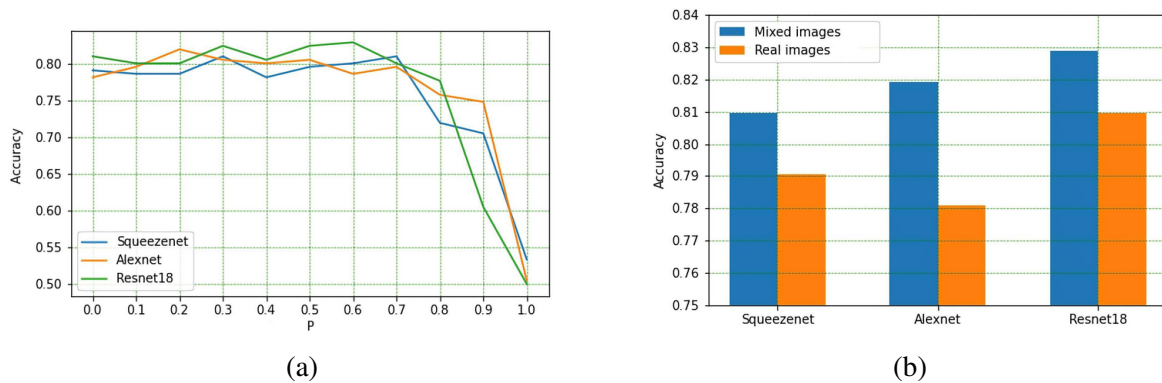


Figure 6: Accuracy over the test set for different percentages of synthetic image for augmentation purposes (a). Accuracy over the test set concerning ResNet18, AlexNet, and SqueezeNet architectures (b).

Table 3: Comparison between human experts and deep models to classify AMD and real Non-AMD images.

	ACC	Sensitivity	Specificity
<b>Clinician #1</b>	0.80	0.80	0.80
<b>Clinician #2</b>	0.75	1.00	0.50
<b>SqueezeNet</b>	0.80	0.80	0.80
<b>AlexNet</b>	0.80	0.70	0.90
<b>Resnet-18</b>	0.85	0.90	0.80

### 3.5. Web Application

The web application was designed to be easy to use and accessed by any user. The application’s home page is minimalist and features a title along with a brief description of its functionality and a button with which the users can upload an image using the “browse” button (Figure 7(a)).

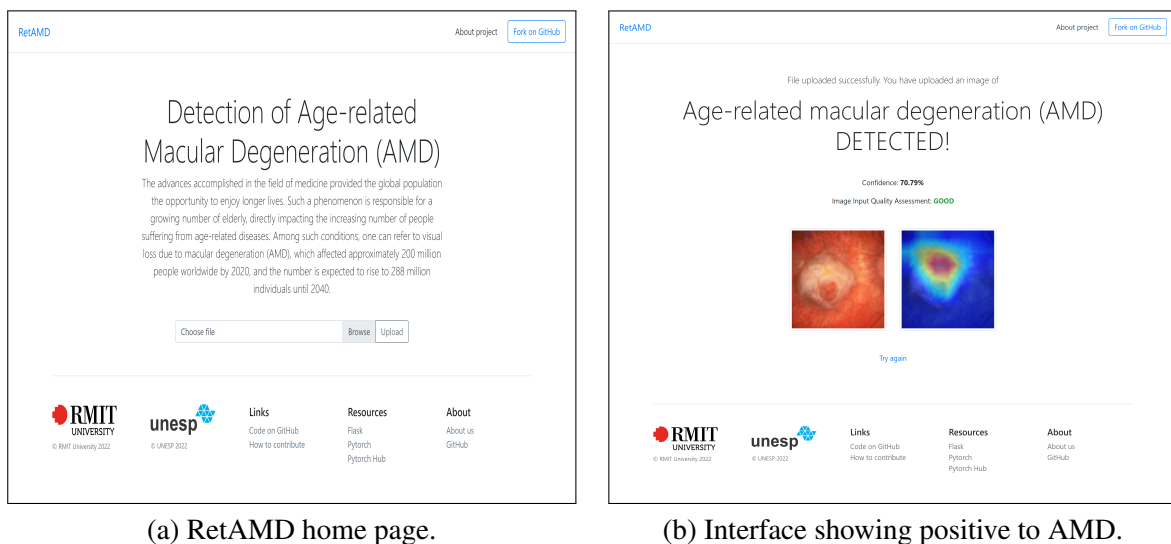


Figure 7: Screenshots.

Once an image file is selected, the system automatically uploads the image to the cloud, performs the

analysis in approximately ten to third seconds (largely based on the internet conditions) displays the output in the form of a figure. The output also informs the user of the success of uploading the file and gives it the label, i.e., AMD detected or not. Additionally, the results also state the level of confidence in the diagnosis and an assessment of the quality of the input image into three quality grades: “Good”, “Usable” and “Reject”.

One of the main issues regarding deep learning in medicine is the difficulty to interpret the decision mechanisms. On the result screen, users can view two images (Figure 7(b)). The uploaded image is displayed on the left and a heatmap created by GradCAM [57] is displayed on the right. This heatmap highlights the regions that were used in the diagnosis and allows the clinical users to understand the basis of the system’s decision. Overall, the results demonstrate the effectiveness and usability of RetAMD in diagnosing AMD.

### 3.6. Model Generalization

The validation of the ResNet18 architecture trained with mixed data ( $p = 0.6$ ) are shown in Table 4 provides the outcomes. The specificity, sensitivity, and accuracy were 80%, 85.7%, and 82.8%, respectively. To test this for generalisability, this deep learning trained model was validated using STARE, a database that was not used during the training phase. 80 images were randomly sampled from STARE; 40 AMD and 40 non-AMD images.

	AMD	Non-AMD
AMD	90	15
Non-AMD	21	84
Specificity	80%	
Sensitivity	85.71%	
Accuracy	82.86%	

Table 4: Confusion matrix in our test set.

	AMD	Non-AMD
AMD	30	10
Non-AMD	5	35
Specificity	87.5%	
Sensitivity	75.0%	
Accuracy	81.25%	

Table 5: Confusion matrix in STARE.

## 4. Discussion

Burlina et al have successfully developed a method for [8, 10] generating the synthetic images. Their method is based on GAN, and they tested their method by showing that experts were unable to identify the synthetic images. However, their method has been patented and hence not available for being used by others. We have introduced an approach that integrates a deep learning quality assessment model and StyleGAN2-ADA, an extension of the progressive GAN. This approach filters out poor-quality retinal images and generates synthetic medical images that human experts are unable to distinguish from real ones. We have also shown that these images were suitable for increase the performance of deep-learning networks. The results were similar to those reported in the literature using patented technology. While Burlina et al. trained a Progressive GAN over a large number of images positive to AMD, our technique has the potential to generate similar high-quality synthetic images with only a small number of images.

Our method has the potential to enhance the approach outlined by Burlina [8, 10]. Assessing image quality could lead to the exclusion of poor-quality images. Additionally, implementing on-the-fly augmentation and selecting the appropriate percentage of synthetic images have shown to be fundamental aspects.

ResNet18 architecture trained over real and synthetic images provided the best results, marginally outperforming the human experts’ performance. While works of Anh et al. [30] report significantly better results, these are all from the same database, with similar equipment used for all the images, images having similar quality and people from the similar ethnic group, which however does not represent the real-world

situation. Our work has shown the potential of using deep learning over multiple datasets where there are differences in people, equipment and image quality.

One limitation of our study is that it has only handled the binary problem, i.e., AMD versus non-AMD images. However, medical images are often non-binary with more classes. While this study and Burlina et al. [8] utilized the expertise of two clinical professionals for image evaluation, it's important to acknowledge that having more experts such as three experts can make the study stronger and tests for the generalisability of the model. Further, three experts permits the disagreements being resolved by voting which tests the strength of the study.

Another limitation of this study is that it used a single-source dataset with 80 images for validation purposes. However, this may be not sufficient to test the model's generalisability.

Different studies have presented results reaching more than 90% accuracy [58, 59]. However, the aim of this study was not to get the best results but for the model to be not limited to any one database. Thus, the focus was on training on a mixed dataset to increase generalization and test this using a different dataset. Another objective was also to develop a web-based tool that provides a model capable of identifying AMD in a wide variety of images from different sources. Our model works on standard CPU computers, which makes it suitable for inexpensive deployment. One limitation in our work is that we have used traditional architectures and not used the number of layers reported nor some recent advances in the state-of-the-art techniques such as used by Anh et al. [30], Grassmann et al. [12], Govindaiah et al. [60], Keel et al. [61], Bhuiyan et al. [62]. This decision was influenced by a common drawback of state-of-the-art convolutional neural networks, which is their complexity. They were typically developed to be trained in extensive datasets, resulting in overfitting when applied to small datasets. However, this study focused on developing a system suitable for being used for web-based applications.

We have made available an online system with this trained network so that anyone can use it and test it, simply by uploading images. The software automatically labels the images as positive or negative to AMD. We have also provided the source code of the entire software and it is available publicly to facilitate researchers to use this as it is, or improve it. We are focused on fostering partnerships to facilitate and conduct research towards the usage of deep-learning to generate and recognize medical images.

The potential of diffusion models [63], known for their advanced capabilities in generating high-quality and diverse images, presents exciting future research in AMD and other ophthalmology diagnoses. These models should be considered for future development.

## 5. Conclusion and Future Works

We have employed a retinal image quality assessment model in preprocessing step. We have compared a number of synthetic medical image generation techniques and found StyleGAN2-ADA to be the most suitable using which we have developed a method to generate synthetic images. We have investigated the use of the synthetic images obtained using examples from publicly available databases to train the model for distinguishing between AMD and healthy eyes. We found that experienced clinical experts were unable to differentiate between synthetic and real images. We have tested the model for generalisability by training the model using images from three databases and validated it using a fourth database. We also have demonstrated that the classification accuracy of deep learning networks marginally outperformed clinical experts in separating the AMD and Non-AMD retinal images.

We have made the source code for generating the synthetic images publicly available to facilitate joint research in the field. We have also provided free access through this paper for the online use of the AMD detection model. This will facilitate future work to broaden the scope for detecting the severity of AMD,

and for differentiating from other diseases. For generating synthetic medical images, there is the need to consider a broader range of deep architectures and the effectiveness of heatmaps helping the clinicians.

## 6. Data availability

The iChallenge-AMD dataset can be found in <https://ai.baidu.com/broad/introduction?dataset=amd>, while ODIR-2019 dataset is available on <https://odir2019.grand-challenge.org/dataset/> and **RIADD** is available on <https://riadd.grand-challenge.org/Home/>.

## 7. Code availability

The official code for StyleGAN2-ADA is available at <https://github.com/NVLabs/stylegan2-ada-pytorch>. Our implementation of Deep Convolutional GAN (DCGAN), Least Squares Generative Adversarial Networks (LSGAN), Wasserstein GAN (WGAN), Wasserstein GAN with Gradient Penalty (WGAN-GP), Deep Regret Analytic Generative Adversarial Networks (DRAGAN), Energy-based Generative Adversarial Network (EBGAN), Boundary Equilibrium Generative Adversarial Networks (BEGAN), Conditional GAN (CGAN), and Auxiliary classifier GAN (ACGAN) are available for download at <https://github.com/GuiCamargoX/gans-pytorch>. All source code concerning image processing, Style-GAN2-ADA data generation, and the pre-trained networks are available at <https://github.com/GuiCamargoX/synthetic-retina-amd>. The web application can be found in <https://amdfundus.space/>. The official Flask code of is available for download in <https://github.com/GuiCamargoX/RetAMD>.

## Author Information

### 7.1. Contributions

G.O. developed the algorithms and performed the analysis. J.P. and D.K. conceptualized and designed the project. G.R., L.P., D.P. managed the data and designed the software. H.K. was responsible for the clinical assessment of the images and script. All authors contributed to writing the manuscript. D.K, G.O. and JP finalized the manuscript.

## Conflict of Interest declarations

The authors declare no conflict of interest for this manuscript.

## Acknowledgment

The authors thank Dr. Ione F. Alexim from BP Hospital - *A Beneficência Portuguesa de São Paulo*, who provided her eye fundus grading expertise to the project. We are grateful to São Paulo Research Foundation (FAPESP) under the grants #2013/07375-0, #2014/12236-1, #2018/15597-6, #2019/00585-5, #2019/07665-4, #2019/02205-5, and #2023/10823-6, to the Brazilian National Council for Research and Development (CNPq) grants #307066/2017-7, #427968/2018-6, #309439/2020-5, and #88887.606573/2021-00, as well as the Engineering and Physical Sciences Research Council (EPSRC) grant EP/T021063/1 and its principal investigator Ahsan Adeel. We also acknowledge the funding from Promobilia Foundation, Sweden, and SPARC grant (P-134, 2019), Department of Biotechnology (India) for financial their support.

## References

- [1] Varun Gulshan, Lily Peng, Marc Coram, Martin C Stumpe, Derek Wu, Arunachalam Narayanaswamy, Subhashini Venugopalan, Kasumi Widner, Tom Madams, Jorge Cuadros, et al. Development and validation of a deep learning algorithm for detection of diabetic retinopathy in retinal fundus photographs. *Jama*, 316(22):2402–2410, 2016.
- [2] Gwénéolé Quéléec, Katia Charrière, Yassine Boudi, Béatrice Cochener, and Mathieu Lamard. Deep image mining for diabetic retinopathy screening. *Medical image analysis*, 39:178–193, 2017.
- [3] Rishab Gargeya and Theodore Leng. Automated identification of diabetic retinopathy using deep learning. *Ophthalmology*, 124(7):962–969, 2017.
- [4] Jeffrey De Fauw, Joseph R Ledsam, Bernardino Romera-Paredes, Stanislav Nikolov, Nenad Tomasev, Sam Blackwell, Harry Askham, Xavier Glorot, Brendan O’Donoghue, Daniel Visentin, et al. Clinically applicable deep learning for diagnosis and referral in retinal disease. *Nature medicine*, 24(9):1342–1350, 2018.
- [5] Parham Khojasteh, Behzad Aliahmad, Sridhar P Arjunan, and Dinesh Kant Kumar. Introducing a novel layer in convolutional neural network for automatic identification of diabetic retinopathy. In *2018 40th Annual International Conference of the IEEE Engineering in Medicine and Biology Society (EMBC)*, pages 5938–5941. IEEE, 2018.
- [6] James M Brown, J Peter Campbell, Andrew Beers, Ken Chang, Susan Ostmo, RV Paul Chan, Jennifer Dy, Deniz Erdogmus, Stratis Ioannidis, Jayashree Kalpathy-Cramer, et al. Automated diagnosis of plus disease in retinopathy of prematurity using deep convolutional neural networks. *JAMA ophthalmology*, 136(7):803–810, 2018.
- [7] Parham Khojasteh, Leandro Aparecido Passos, Tiago Carvalho, Edmar Rezende, Behzad Aliahmad, João Paulo Papa, and Dinesh Kant Kumar. Exudate detection in fundus images using deeply-learnable features. *Computers in biology and medicine*, 104:62–69, 2019.
- [8] Philippe M Burlina, Neil Joshi, Katia D Pacheco, TY Alvin Liu, and Neil M Bressler. Assessment of deep generative models for high-resolution synthetic retinal image generation of age-related macular degeneration. *JAMA ophthalmology*, 137(3):258–264, 2019.
- [9] Philippe M Burlina, Neil Joshi, Michael Pekala, Katia D Pacheco, David E Freund, and Neil M Bressler. Automated grading of age-related macular degeneration from color fundus images using deep convolutional neural networks. *JAMA ophthalmology*, 135(11):1170–1176, 2017.
- [10] Phillippe Burlina, Neil Joshi, Katia D Pacheco, David E Freund, Jun Kong, and Neil M Bressler. Utility of deep learning methods for referability classification of age-related macular degeneration. *JAMA ophthalmology*, 136(11):1305–1307, 2018.
- [11] Philippe M Burlina, Neil Joshi, Katia D Pacheco, David E Freund, Jun Kong, and Neil M Bressler. Use of deep learning for detailed severity characterization and estimation of 5-year risk among patients with age-related macular degeneration. *JAMA ophthalmology*, 136(12):1359–1366, 2018.
- [12] Felix Grassmann, Judith Mengelkamp, Caroline Brandl, Sebastian Harsch, Martina E Zimmermann, Birgit Linkohr, Annette Peters, Iris M Heid, Christoph Palm, and Bernhard HF Weber. A deep learning algorithm for prediction of age-related eye disease study severity scale for age-related macular degeneration from color fundus photography. *Ophthalmology*, 125(9):1410–1420, 2018.
- [13] Andre Esteva, Alexandre Robicquet, Bharath Ramsundar, Volodymyr Kuleshov, Mark DePristo, Katherine Chou, Claire Cui, Greg Corrado, Sebastian Thrun, and Jeff Dean. A guide to deep learning in healthcare. *Nature medicine*, 25(1):24–29, 2019.
- [14] H Fu, F Li, Ji Orlando, H Bogunovic, X Sun, J Liao, Y Xu, S Zhang, and X Zhang. Adam: Automatic detection challenge on age-related macular degeneration. *IEEE Dataport*, 2020.
- [15] Parham Khojasteh, Behzad Aliahmad, and Dinesh K Kumar. Fundus images analysis using deep features for detection of exudates, hemorrhages and microaneurysms. *BMC ophthalmology*, 18(1):1–13, 2018.
- [16] Parham Khojasteh, Behzad Aliahmad, and Dinesh Kant Kumar. A novel color space of fundus images for automatic exudates detection. *Biomedical signal processing and control*, 49:240–249, 2019.
- [17] Lorenzo Brigato and Luca Iocchi. A close look at deep learning with small data. In *2020 25th International Conference on Pattern Recognition (ICPR)*, pages 2490–2497. IEEE, 2021.
- [18] Luis Perez and Jason Wang. The effectiveness of data augmentation in image classification using deep learning. *arXiv preprint arXiv:1712.04621*, 2017.
- [19] Ian J Goodfellow, Jean Pouget-Abadie, Mehdi Mirza, Bing Xu, David Warde-Farley, Sherjil Ozair, Aaron Courville, and Yoshua Bengio. Generative adversarial networks. *arXiv preprint arXiv:1406.2661*, 2014.
- [20] Maayan Frid-Adar, Idit Diamant, Eyal Klang, Michal Amitai, Jacob Goldberger, and Hayit Greenspan. Gan-based synthetic medical image augmentation for increased cnn performance in liver lesion classification. *Neurocomputing*, 321:321–331, 2018.
- [21] Luis A Souza Jr, Leandro A Passos, Robert Mendel, Alanna Ebigbo, Andreas Probst, Helmut Messmann, Christoph Palm, and João P Papa. Assisting barrett’s esophagus identification using endoscopic data augmentation based on generative adversarial networks. *Computers in Biology and Medicine*, page 104029, 2020.

- [22] Luis A Souza Jr, Leandro A Passos, Robert Mendel, Alanna Ebigbo, Andreas Probst, Helmut Messmann, Christoph Palm, and João P Papa. Fine-tuning generative adversarial networks using metaheuristics: A case study on barrett’s esophagus identification. In *Bildverarbeitung für die Medizin 2021. Proceedings, German Workshop on Medical Image Computing, Regensburg, March 7-9, 2021*, pages 205–210. Springer Vieweg, 2021.
- [23] Hojjat Salehinejad, Shahrokh Valaee, Tim Dowdell, Errol Colak, and Joseph Barfett. Generalization of deep neural networks for chest pathology classification in x-rays using generative adversarial networks. In *2018 IEEE International Conference on Acoustics, Speech and Signal Processing (ICASSP)*, pages 990–994. IEEE, 2018.
- [24] Xintao Wang, Ke Yu, Shixiang Wu, Jinjin Gu, Yihao Liu, Chao Dong, Yu Qiao, and Chen Change Loy. Esrgan: Enhanced super-resolution generative adversarial networks. In *Proceedings of the European conference on computer vision (ECCV) workshops*, pages 0–0, 2018.
- [25] Kaveri A Thakoor, Ari Carter, Ge Song, Adam Wax, Omar Moussa, Royce WS Chen, Christine Hendon, and Paul Sajda. Enhancing portable oct image quality via gans for ai-based eye disease detection. In *International Workshop on Distributed, Collaborative, and Federated Learning*, pages 155–167. Springer, 2022.
- [26] Vineeta Das, Samarendra Dandapat, and Prabin Kumar Bora. Unsupervised super-resolution of oct images using generative adversarial network for improved age-related macular degeneration diagnosis. *IEEE Sensors Journal*, 20(15):8746–8756, 2020.
- [27] Tao Li, Wang Bo, Chunyu Hu, Hong Kang, Hanruo Liu, Kai Wang, and Huazhu Fu. Applications of deep learning in fundus images: A review. *Medical Image Analysis*, 69:101971, 2021.
- [28] Valentina Bellemo, Philippe Burlina, Liu Yong, Tien Yin Wong, and Daniel Shu Wei Ting. Generative adversarial networks (gans) for retinal fundus image synthesis. In *Asian Conference on Computer Vision*, pages 289–302. Springer, 2018.
- [29] Tero Karras, Timo Aila, Samuli Laine, and Jaakko Lehtinen. Progressive growing of gans for improved quality, stability, and variation. *arXiv preprint arXiv:1710.10196*, 2017.
- [30] Sangil Ahn, Su Jeong Song, and Jitae Shin. Fundusgan: Fundus image synthesis based on semi-supervised learning. *Biomedical Signal Processing and Control*, 86:105289, 2023.
- [31] Veena Mayya, Uma Kulkarni, Divyalakshmi Kaiyoor Surya, and U Rajendra Acharya. An empirical study of preprocessing techniques with convolutional neural networks for accurate detection of chronic ocular diseases using fundus images. *Applied Intelligence*, 53(2):1548–1566, 2023.
- [32] Zhaoran Wang, Gilbert Lim, Wei Yan Ng, Tien-En Tan, Jane Lim, Sing Hui Lim, Valencia Foo, Joshua Lim, Laura Gutierrez Sinisterra, Feihui Zheng, et al. Synthetic artificial intelligence using generative adversarial network for retinal imaging in detection of age-related macular degeneration. *Frontiers in Medicine*, 10:1184892, 2023.
- [33] Yoga Advaita Veturi, William Woof, Teddy Lazebnik, Ismail Moghul, Peter Woodward-Court, Siegfried K Wagner, Thales Antonio Cabral de Guimarães, Malena Daich Varela, Bart Liefers, Praveen J Patel, et al. Syntheye: Investigating the impact of synthetic data on artificial intelligence-assisted gene diagnosis of inherited retinal disease. *Ophthalmology Science*, 3(2):100258, 2023.
- [34] Jost B Jonas. Global prevalence of age-related macular degeneration. *The Lancet Global Health*, 2(2):e65–e66, 2014.
- [35] Wan Ling Wong, Xinyi Su, Xiang Li, Chui Ming G Cheung, Ronald Klein, Ching-Yu Cheng, and Tien Yin Wong. Global prevalence of age-related macular degeneration and disease burden projection for 2020 and 2040: a systematic review and meta-analysis. *The Lancet Global Health*, 2(2):e106–e116, 2014.
- [36] Patricia T Harvey. Common eye diseases of elderly people: identifying and treating causes of vision loss. *Gerontology*, 49(1):1–11, 2003.
- [37] Huazhu Fu, Boyang Wang, Jianbing Shen, Shanshan Cui, Yanwu Xu, Jiang Liu, and Ling Shao. Evaluation of retinal image quality assessment networks in different color-spaces. In *International Conference on Medical Image Computing and Computer-Assisted Intervention*, pages 48–56. Springer, 2019.
- [38] Tero Karras, Miika Aittala, Janne Hellsten, Samuli Laine, Jaakko Lehtinen, and Timo Aila. Training generative adversarial networks with limited data. In *Proc. NeurIPS*, 2020.
- [39] Samiksha Pachade, Prasanna Porwal, Dhanshree Thulkar, Manesh Kokare, Girish Deshmukh, Vivek Sahasrabuddhe, Luca Giancardo, Gwenolé Quellec, and Fabrice Mériaudeau. Retinal fundus multi-disease image dataset (rfmid): A dataset for multi-disease detection research. *Data*, 6(2):14, 2021.
- [40] Martin Heusel, Hubert Ramsauer, Thomas Unterthiner, Bernhard Nessler, and Sepp Hochreiter. Gans trained by a two time-scale update rule converge to a local nash equilibrium. *Advances in neural information processing systems*, 30, 2017.
- [41] Alec Radford, Luke Metz, and Soumith Chintala. Unsupervised representation learning with deep convolutional generative adversarial networks. *arXiv preprint arXiv:1511.06434*, 2015.
- [42] Xudong Mao, Qing Li, Haoran Xie, Raymond YK Lau, Zhen Wang, and Stephen Paul Smolley. Least squares generative adversarial networks. In *Proceedings of the IEEE international conference on computer vision*, pages 2794–2802, 2017.
- [43] Martin Arjovsky, Soumith Chintala, and Léon Bottou. Wasserstein generative adversarial networks. In *International conference on machine learning*, pages 214–223. PMLR, 2017.

- [44] Ishaan Gulrajani, Faruk Ahmed, Martin Arjovsky, Vincent Dumoulin, and Aaron Courville. Improved training of wasserstein gans. *arXiv preprint arXiv:1704.00028*, 2017.
- [45] Naveen Kodali, Jacob Abernethy, James Hays, and Zsolt Kira. On convergence and stability of gans. *arXiv preprint arXiv:1705.07215*, 2017.
- [46] Junbo Zhao, Michael Mathieu, and Yann LeCun. Energy-based generative adversarial network. *arXiv preprint arXiv:1609.03126*, 2016.
- [47] David Berthelot, Thomas Schumm, and Luke Metz. Began: Boundary equilibrium generative adversarial networks. *arXiv preprint arXiv:1703.10717*, 2017.
- [48] Mehdi Mirza and Simon Osindero. Conditional generative adversarial nets. *arXiv preprint arXiv:1411.1784*, 2014.
- [49] Augustus Odena, Christopher Olah, and Jonathon Shlens. Conditional image synthesis with auxiliary classifier gans. In *International conference on machine learning*, pages 2642–2651. PMLR, 2017.
- [50] Diederik P. Kingma and Jimmy Ba. Adam: A method for stochastic optimization, 2017.
- [51] Jia Deng, Wei Dong, Richard Socher, Li-Jia Li, Kai Li, and Li Fei-Fei. Imagenet: A large-scale hierarchical image database. In *2009 IEEE conference on computer vision and pattern recognition*, pages 248–255. Ieee, 2009.
- [52] Forrest N Iandola, Song Han, Matthew W Moskewicz, Khalid Ashraf, William J Dally, and Kurt Keutzer. Squeezenet: Alexnet-level accuracy with 50x fewer parameters and; 0.5 mb model size. *arXiv preprint arXiv:1602.07360*, 2016.
- [53] Alex Krizhevsky, Ilya Sutskever, and Geoffrey E Hinton. Imagenet classification with deep convolutional neural networks. *Advances in neural information processing systems*, 25:1097–1105, 2012.
- [54] Kaiming He, Xiangyu Zhang, Shaoqing Ren, and Jian Sun. Deep residual learning for image recognition. In *Proceedings of the IEEE conference on computer vision and pattern recognition*, pages 770–778, 2016.
- [55] Pavlos Efraimidis and Paul Spirakis. Weighted random sampling. In Ming-Yang Kao, editor, *Encyclopedia of Algorithms*, pages 1024–1027, Boston, MA, 2008. Springer US.
- [56] Adam Paszke, Sam Gross, Francisco Massa, Adam Lerer, James Bradbury, Gregory Chanan, Trevor Killeen, Zeming Lin, Natalia Gimelshein, Luca Antiga, et al. Pytorch: An imperative style, high-performance deep learning library. *Advances in neural information processing systems*, 32, 2019.
- [57] Ramprasaath R Selvaraju, Michael Cogswell, Abhishek Das, Ramakrishna Vedantam, Devi Parikh, and Dhruv Batra. Grad-cam: Visual explanations from deep networks via gradient-based localization. In *Proceedings of the IEEE international conference on computer vision*, pages 618–626, 2017.
- [58] Emma Pead, Roly Megaw, James Cameron, Alan Fleming, Baljean Dhillon, Emanuele Trucco, and Thomas MacGillivray. Automated detection of age-related macular degeneration in color fundus photography: a systematic review. *survey of ophthalmology*, 64(4):498–511, 2019.
- [59] Xiangjie Leng, Ruijie Shi, Yanxia Wu, Shiyin Zhu, Xingcan Cai, Xuejing Lu, and Ruobing Liu. Deep learning for detection of age-related macular degeneration: A systematic review and meta-analysis of diagnostic test accuracy studies. *Plos one*, 18(4):e0284060, 2023.
- [60] Arun Govindaiah, Roland Theodore Smith, and Alauddin Bhuiyan. A new and improved method for automated screening of age-related macular degeneration using ensemble deep neural networks. In *2018 40th Annual international conference of the IEEE engineering in medicine and biology society (EMBC)*, pages 702–705. IEEE, 2018.
- [61] Stuart Keel, Zhixi Li, Jane Scheetz, Liubov Robman, James Phung, Galina Makeyeva, KhinZaw Aung, Chi Liu, Xixi Yan, Wei Meng, et al. Development and validation of a deep-learning algorithm for the detection of neovascular age-related macular degeneration from colour fundus photographs. *Clinical & Experimental Ophthalmology*, 47(8):1009–1018, 2019.
- [62] Alauddin Bhuiyan, Tien Yin Wong, Daniel Shu Wei Ting, Arun Govindaiah, Eric H Souied, and R Theodore Smith. Artificial intelligence to stratify severity of age-related macular degeneration (amd) and predict risk of progression to late amd. *Translational vision science & technology*, 9(2):25–25, 2020.
- [63] Florinel-Alin Croitoru, Vlad Hondru, Radu Tudor Ionescu, and Mubarak Shah. Diffusion models in vision: A survey. *IEEE Transactions on Pattern Analysis and Machine Intelligence*, 2023.